

# **APPLICATION OF MULTIGRID CORRECTION SCHEME TO NONLINEAR NODAL METHOD SOLUTIONS WITH USE OF CORE REFLECTOR BOUNDARY CONDITIONS**

Ku Young Chung and Chang Hyo Kim  
Department of Nuclear Engineering  
Seoul National University  
niro90@snu.ac.kr ; kchyong@gong.snu.ac.kr

## **ABSTRACT**

This paper discusses effectiveness of the core-reflector boundary conditions(CRBC) and the two grid correction(TGC) scheme in enhancing the computational efficiency of the nonlinear nodal methods. In doing so, the CRBC is incorporated into the coarse mesh finite difference(CMFD) formulation based on two-node nodal expansion method(NEM) and the analytical nodal method(ANM). The TGC scheme which utilizes one-node-per-assembly(1 N/FA) three dimensional(3D) coarse grid equations to speed up the bi-conjugate gradient stabilized (BiCGSTAB) iterative solutions of the four-node-per-assembly(4 N/FA) 3D NEM and ANM CMFD equations for the OECD/NEA PWR transient problems is described along with the specification of the restriction and the prolongation matrices. The effects of the TGC scheme as well as the CRBC on the efficiency of the CMFD solutions are then presented in terms of the 4 N/FA NEM and ANM analysis for the slow and fast transients in the OECD/NEA PWR. It is demonstrated that the CRBC and the TGC scheme can achieve the CPU time saving of about 40 %.

## **1. INTRODUCTION**

Nonlinear nodal methods have enhanced significantly efficiency of the NEM or ANM solutions of the static and transient reactor physics problems<sup>1,2</sup>. There are rooms to enhance further their efficiency in solving reactor physics problems. One is to incorporate the CRBC<sup>3</sup> into the nodal CMFD formulation, as we demonstrated in terms of 1 N/FA NEM and ANM solutions to OECD/NEA PWR transient benchmark problems<sup>4,5</sup>. Another is to adopt the multigrid correction scheme for acceleration of the CMFD solution<sup>6,7</sup>.

The performance of multigrid method for neutron diffusion equation was first tested by Alcouffe<sup>8</sup>. He introduced a multigrid scheme for solving two-dimensional two group finite difference diffusion equation. Zaslavsky<sup>9</sup> introduced algebraic multigrid scheme for reactor criticality calculation. His algebraic multigrid scheme constructs coarse grid equation and restriction operator using fine grid matrix elements without geometric grid informations. This scheme is

usually adopted when the geometric multigrid scheme is not readily implemented. Scheichl<sup>10</sup> presented a parallel solver for NEM with parallel multigrid scheme. Rifat M. Al-Chalabi and Paul J. Turinsky<sup>11</sup> presented testing of a multigrid scheme for CMFD NEM based steady-state core analysis without giving explicit details on the number of levels, grid size for each level, the cycle design, etc. In this paper, we introduce TGC scheme for the acceleration of 3-D 4 N/A CMFD NEM and ANM solutions to OECD/NEA PWR transient benchmark problem. Also, we will suggest restriction and prolongation matrices that we have found very efficient in speeding up the CMFD of NEM and ANM solution.

We will demonstrate that adoption of TGC as well as use of the CRBC can achieve more than 40 % CPU time reduction in obtaining 4 N/FA NEM and ANM solutions to most of the OECD/NEA PWR transient benchmark problems<sup>12,13</sup>.

## 2. INCORPORATION OF CRBC INTO CMFD FORMULATION

The CMFD formulation requires solving the transverse integrated one-dimensional two-group diffusion equation of the following form<sup>14</sup>:

$$\begin{aligned}
& -D_g^{(n)} \frac{d^2}{du^2} \Phi_g^{(n)}(u) + \Sigma_{tg}^{(n)} \Phi_g^{(n)}(u) \\
& = \left[ \sum_{g'} \Sigma_{g'g}^{(n)} \Phi_{g'}^{(n)} + \kappa_g \Phi^{(n)}(u) - L_{gv}^{(n)}(u) - L_{gw}^{(n)}(u) + S_{ext,g}^{(n)}(u) \right] \\
& + \left( \kappa_g \left[ (A^{(n)} - \beta) \psi^{(n)}(u) + B^{(n)} \psi^{(n-1)} \right] + C^{(n-1)} f_g \{ C_i^{(n-1)}(u) \} \right) \\
& \left. + \frac{1}{v_g \Delta t_n} \left[ \Phi_g^{(n-1)}(u) - \Phi_g^{(n)}(u) \right] \right)
\end{aligned} \quad (1)$$

For the core interior nodes, Eq. (1) defines a two-node problem. For the core periphery nodes facing the reflectors, however, it reduces to one-node problem with the use of CRBC<sup>3</sup>,

$$\mathbf{J}_u^{(n)} = \mathbf{R} \mathbf{F}^{(n)} + \mathbf{P} \mathbf{L}_u^{(n)} + \mathbf{Q} \mathbf{J}_v^{(n)} \quad (2)$$

where  $\mathbf{J}_x^{(n)}$  ( $x=u,v$ ),  $\mathbf{F}^{(n)}$ , and  $\mathbf{L}_u^{(n)}$  are two-dimensional column vectors constructed with two group x-directed net currents ( $J_{gu}^{(n)}$ ), fluxes ( $\Phi_{gu}^{(n)}$ ), and transverse leakages ( $L_{gu}^{(n)}$ ) at the core reflector boundaries at the time step n, respectively. The  $\mathbf{R}$ ,  $\mathbf{P}$ , and  $\mathbf{Q}$  are 2x2 matrices whose elements are defined in Ref. 3 in terms of two group constants of the reflector.

In the NEM CMFD formulation, Eq. (1) is approximately solved by assuming the forth-order polynomial form of solutions for  $\Phi_g^{(n)}(u)$ ;

$$\Phi_g^{(n)}(u) = C_{0gu}^{(n)} h_0(u) + C_{1gu}^{(n)} h_1(u) + C_{2gu}^{(n)} h_2(u) + C_{3gu}^{(n)} h_3(u) + C_{4gu}^{(n)} h_4(u), \quad (3)$$

where the polynomial expansion functions  $h_i(u)$ 's are defined in Ref. 15. Four expansion coefficients per each group ( $C_{igu}^{(n)}$ ;  $i=1,2,3,4$ ) in one node problem are determined using the flux and current continuity conditions and three flux moment equations for the boundary node that are obtained by applying the weighted residual method to Eq. (1) with  $h_i(u)$  ( $i=0,1,2$ ).

In the ANM CMFD formulation, Eq. (1) is solved analytically in the following form<sup>2</sup> ;

$$\begin{pmatrix} \Phi_1^{(n)}(\mathbf{u}) \\ \Phi_2^{(n)}(\mathbf{u}) \end{pmatrix} = \begin{pmatrix} r & s \\ 1 & 1 \end{pmatrix} \begin{pmatrix} a_{21}\text{sn}(\kappa\mathbf{u}) + a_{22}\text{cn}(\kappa\mathbf{u}) \\ a_{23}\text{sn}(\mu\mathbf{u}) + a_{24}\text{cn}(\mu\mathbf{u}) \end{pmatrix} + \begin{pmatrix} c_{10} + c_{11}f_1(\mathbf{u}) + c_{12}f_2(\mathbf{u}) \\ c_{20} + c_{21}f_1(\mathbf{u}) + c_{22}f_2(\mathbf{u}) \end{pmatrix}. \quad (4)$$

The four unknown coefficients of Eq. (4) for the boundary node,  $a_{ij}$  ( $i,j=1,2$ ), are determined by the node average flux constraints for each group and the flux and the current continuity at the core-reflector boundary. Mathematical details for the NEM and ANM CMFD in the boundary node are available in Refs. 4 and 5.

Once the  $\Phi_g^{(n)}(\mathbf{u})$  is obtained, the net current  $J_{gu}^{(n)} = -D_g^{(n)} \frac{\partial}{\partial \mathbf{u}} \Phi_g^{(n)}$  is used to update the corrective diffusion coefficient,  $D_{gu}^N$ , in the CMFD equation for the boundary node by

$$J_{gu}^{(n)} = -D_{gu}^F \left( \Phi_g^{(n)} - \overline{\Phi_g^{(n)}} \right) - D_{gu}^N \left( \Phi_g^{(n)} + \overline{\Phi_g^{(n)}} \right). \quad (5)$$

### 3. MULTIGRID CORRECTION SCHEME

The multigrid correction(MGC) scheme is an acceleration method for the speedy reduction of slowly decreasing global error terms in the iterative solution process of a given system of equations by making use of the correction that can be derivable from coarse grid equations corresponding to the given system of equations. The general description of the MGC schemes is available in Ref. 6. Here we describe briefly the TGC scheme that we adopted in this paper.

Suppose that we seek a 4 N/FA ANM or NEM solution of the given neutronics benchmark problems. Then it becomes necessary to solve the ANM or NEM CMFD equations corresponding to the 4 N/FA discretization of the following form,

$$\mathbf{A}_f \mathbf{F}_f = \mathbf{b}_f. \quad (6)$$

Without the multigrid correction, all one has to do is to solve this equation using a currently popular iterative solution method called Bi-CGSTAB<sup>16</sup> method till the solution vector converges. In the TGC scheme, we use the interim solution,  $F_f^{(p)}$ , that one can get after the p-th iteration step of the Bi-CGSTAB method for Eq. (6). The interim solution contains the error designated by  $\mathbf{e}_f^{(p)}$ , which satisfies

$$\mathbf{A}_f \mathbf{e}_f^{(p)} = \mathbf{r}_f^{(p)} \quad (7)$$

where the residual vector  $\mathbf{r}_f^{(p)}$  is given by  $\mathbf{b}_f - \mathbf{A}_f F_f^{(p)}$ . The error,  $\mathbf{e}_f^{(p)}$ , may contain slowly reducing global error components which we hope to remove speedily by correcting with a coarse grid error vector. To implement this, let's consider the 1 N/FA coarse grid equations corresponding to Eq. (6),

$$\mathbf{A}_c \mathbf{F}_c = \mathbf{b}_c. \quad (8)$$

From Eq. (8), one can constitute the coarse grid residual equation,

$$\mathbf{A}_c \mathbf{e}_c^{(p)} = \mathbf{r}_c^{(p)}. \quad (9)$$

For correction of  $F_f^{(p)}$ , we put  $\mathbf{r}_c^{(p)} = \mathbf{R} \mathbf{r}_f^{(p)}$  in which the  $\mathbf{R}$  is the restriction matrix which converts fine grid residual vector to coarse grid residual vector. Solving Eq. (9) with  $\mathbf{r}_c^{(p)}$ , one can

obtain the coarse grid error vector  $\mathbf{e}_c^{(p)}$ . One can then find the fine grid error vector by  $\mathbf{e}_f^{(p)} = \mathbf{P}\mathbf{e}_c^{(p)}$  in which the  $\mathbf{P}$  is the prolongation matrix which converts the coarse grid error to the fine grid error. The  $F_f^{(p)}$  is then corrected by  $\mathbf{e}_f^{(p)}$ . Table I summarizes the TGC scheme.

Table I. Two Grid Correction Scheme

<ol style="list-style-type: none"> <li>1) Solve <math>\mathbf{A}_f F_f = \mathbf{b}_f</math> iteratively to obtain the <math>p^{\text{th}}</math> step solution <math>F_f^{(p)}</math></li> <li>2) Set <math>\mathbf{r}_f^{(p)} = \mathbf{b}_f - \mathbf{A}_f F_f^{(p)}</math></li> <li>3) Set <math>\mathbf{r}_c^{(p)} = \mathbf{R}\mathbf{r}_f^{(p)}</math></li> <li>4) Solve <math>\mathbf{A}_c \mathbf{e}_c^{(p)} = \mathbf{r}_c^{(p)}</math> approximately</li> <li>5) Set <math>\mathbf{e}_f^{(p)} = \mathbf{P}\mathbf{e}_c^{(p)}</math></li> <li>6) Set <math>F_f^{(p)} = F_f^{(p)} + \mathbf{e}_f^{(p)}</math></li> <li>7) If <math>F_f^{(p)}</math> is not converged, go to step 1). Otherwise stop.</li> </ol>
--

The performance of TGC scheme is largely dependent on selection of restriction and prolongation matrices. Appropriate restriction and prolongation matrices guarantee the effective removal of global error components and speedy convergence of iterative solution. To define restriction matrix, we note that fine grid fluxes may be related to the coarse grid flux

$\Phi_c = \frac{1}{4}(\Phi_f^{\text{ul}} + \Phi_f^{\text{ur}} + \Phi_f^{\text{dl}} + \Phi_f^{\text{dr}})$  (Cf. Fig. 1). In analogy to this relation, we assume that the coarse grid residual is related to fine grid residuals as  $r_c = \frac{1}{4}(r_f^{\text{ul}} + r_f^{\text{ur}} + r_f^{\text{dl}} + r_f^{\text{dr}})$  where  $r_f^m$  ( $m=\text{ul,ur,dl,dr}$ ) are the residual components associated with the fine grid flux  $\Phi_f^m$ .

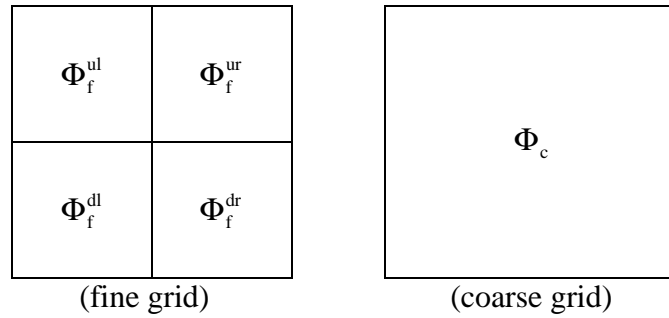


Figure 1. Fine Grid and Coarse Grid

The prolongation matrix is often defined by the transpose of restriction matrix<sup>6)</sup>. In this paper, however, we defined differently. Prolongation is interpreted as the reconstruction process from coarse grid nodal flux to fine grid one. We assumed that fine grid flux shape is preserved even after the correction. This assumption corresponds to putting  $\mathbf{e}_f^m = \frac{\Phi_f^m}{\Phi_c} \mathbf{e}_c$ .

#### 4. NUMERICAL RESULTS AND DISCUSSION

The effects of the TGC scheme as well as the CRBC on the efficiency of the CMFD solution are examined in terms of 4 N/FA NEM and ANM analysis for the fast and slow transients in OECD/NEA PWR. Table II summarizes the effect of the CRBC on the efficiency of the CMFD ANM and NEM solutions. Table III and IV show the effect of the TGC scheme on the CMFD solutions. The CMFD solutions with and without explicit representation of reflectors are parenthesized with E and B, respectively.

Table II shows that the 4 N/FA CMFD ANM(E) and NEM(E) solutions compare very well with the reference PANTHER calculations<sup>17,18</sup> in prediction of steady state critical soluble boron concentration, power peak, and key transient parameters. It also shows that replacement of reflectors by the CRBC affects very little the prediction accuracy of the CMFD solutions in all the transient cases but that the use of the CRBC reduces 20 to 30 % CPU time, depending on the transient cases.

Table III and IV display the CPU time reductions made by incorporating the TGC scheme into the Bi-CGSTAB iterative solution method of the CMFD formulation of the transient benchmark problems. In terms of total CPU time involving neutronics and thermal hydraulic feedback calculations, the TGC scheme is shown to achieve 15 to 25 % CPU time saving. In terms of the CPU time spent on the iterative neutronics calculation alone, the CPU time saving by the TGC scheme is more striking, as noted in Table IV. Actually, the CPU time saving by the TGC scheme depends on the correction frequency. Figure 2 illustrates the effect of the TGC frequency on the gradual reduction of the norm of the residual vector versus the fine grid Bi-CGSTAB iteration step index in the CMFD NEM solutions of the fast transient case A1 and the slow transient case B. As shown vividly in these figures, adoption of the TGC scheme brings down the norm of the residual vector below the prescribed limit within much fewer Bi-CGSTAB iteration steps than otherwise. The reduction trend depends on how frequently one introduces the TGC scheme into the fine grid Bi-CGSTAB iteration process. As observed in Table V, the TGC every two or three Bi-CGSTAB iteration results in the most CPU time saving.

Table V. Effect of Two Grid Correction Frequency on Iteration Step and CPU time

Correction Frequency		NC <sup>a</sup>	TGC(1) <sup>b</sup>	TGC(2) <sup>b</sup>	TGC(3) <sup>b</sup>	TGC(4) <sup>b</sup>
A1	Fine grid iteration step	38	10	8	10	13
	Correction count	0	9	3	3	3
	Coarse grid iteration step	0	66	26	29	31
	CPU time(s) <sup>c</sup>	368.9	357.4	242.4	252.8	268.2
B	Fine grid iteration step	61	9	9	11	14
	Correction count	0	8	4	3	3
	Coarse grid iteration step	0	85	64	55	57
	CPU time(s) <sup>c</sup>	702.3	648.9	485.4	473.0	499.7

<sup>a</sup>No two-grid correction.

<sup>b</sup>The integer  $i(=1,2,3,4)$  in the brackets denotes that the TGC is applied every  $i$  Bi-CGSTAB iterations.

<sup>c</sup>The CPU time spent on iterative neutronics calculation by DEC workstation(433MHz).

The compounding effect of the CRBC and the TGC scheme on the CPU time saving in the

CMFD solutions of OECD/NEA transient benchmark problems is significantly large. Let's take C1 case, for example. The C1 is the most time consuming transient problem because it is a full core transient problem. The CMFD NEM(E) and ANM(E) solution without the TGC scheme require the CPU times of 5674 and 7119 seconds, respectively (cf. Table III) while the CMFD NEM(B) AND ANM(B) solutions with the TGC scheme less than 60 % CPU times, e.g., 3284 and 4112 seconds, respectively. From Tables III and IV, one observes the CPU time saving of the similar order in most of the other benchmark problems.

## CONCLUSIONS

A certain class of reactor transient problems requires the coupled thermal hydraulics and the 3D neutronics kinetics analysis. Considering the heavy computational burden usually involved in such problems, the CPU time saving of about 40 % in neutronics part alone is very significant in enhancing the overall efficiency of the transient analysis and justifies the application of the TGC as well as use of the CRBC. For further efficiency enhancement of neutronics kinetics calculation, parallel computing three-level correction scheme is under investigation.

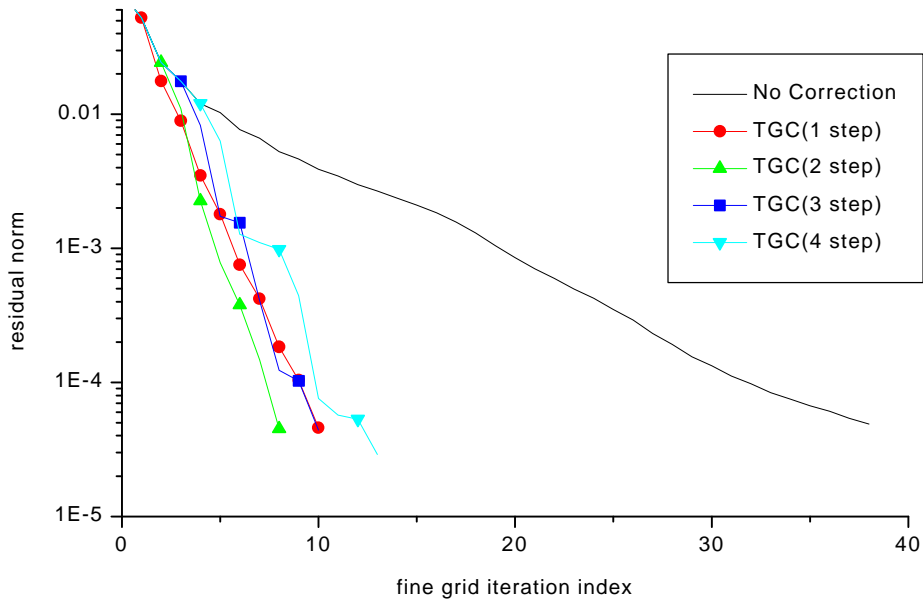
## ACKNOWLEDGEMENTS

This work was supported by Korea Science and Engineering Foundation(KOSEF).

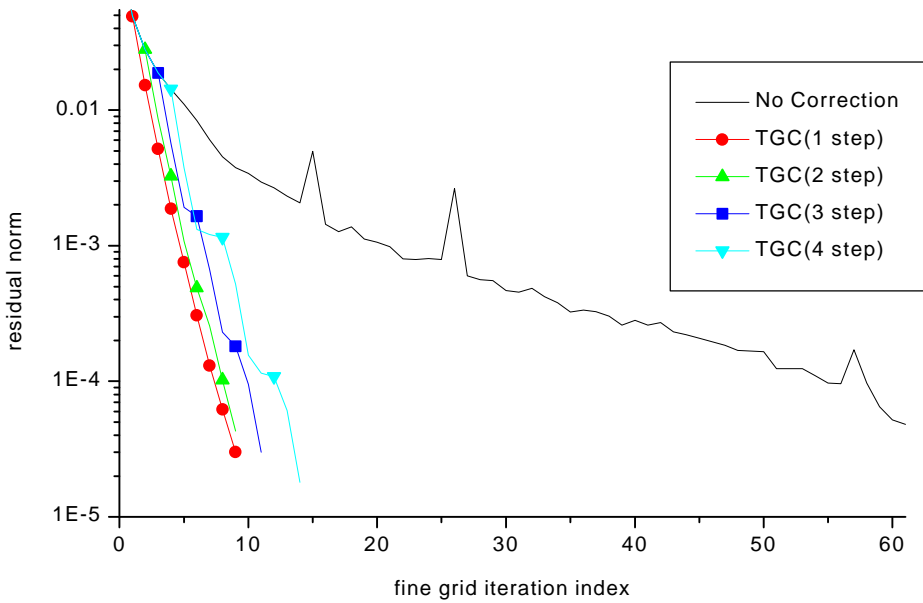
## REFERENCES

1. K. S. Smith, "Nodal Storage Reduction by Nonlinear Iteration," *Trans. Am. Nucl.* Vol. **44**, 265 (1983).
2. H. G. Joo, T. J. Downer, and D. A. Barber, "Parallel Computing Method for the EPRI Spatial Kinetics Code ARROTTA," *Proc. ANS. Top. Mtg - Adv. Nucl. Fuel. Man. II*, Mrytle Beach, S. C., 20.31-20.38 (1997).
3. Eun Ki Lee, Chang Hyo Kim, and Hyung Kook Joo, "New Core-Reflector Boundary Conditions for Transient Nodal Reactor Calculations," *Nucl. Sci. Eng.*, **121**, pp. 114-129 (1995).
4. Chang Hyo Kim, Eun Ki Lee, and Seong Man Bae, "Coarse Mesh Finite Difference Computation With Replacement of Reflectors by Core-Reflector Boundary Conditions," *Proc. Int. Conf. on the Physics of Nuclear Science and Technology*, Oct. 5-8 1998, Long Island, New York, Vol. **2**, pp. 1213-1219.
5. Ku Young Chung, Chang Hyo Kim, and Eun Ki Lee, "Effectiveness of Core-Reflector Boundary Conditions on Transient Nodal Coarse Mesh Finite Difference Method," (To appear in Transactions of 1999 ANS Winter Meeting.)
6. W. L. Briggs, *A Multigrid Tutorial*, SIAM, Philadelphia (1987).

7. C. C. Douglas and J. Douglas, "A unified convergence theory for abstract multigrid or multilevel algorithms, serial and parallel," *SIAM J. Numer. Anal.*, **30**, pp. 136-158 (1993).
8. R. Alcouffe, "The Multigrid Method for Solving the Two-Dimensional Multigroup Diffusion Equation," *Proc. Topl. Mtg. Advances in Reactor Computations*, Salt Lake City, UT, p. 340 (1983).
9. Leonid Yu. Zaslavsky, "An Adaptive Algebraic Multigrid For Reactor Criticality Calculations," *SIAM J. Sci. Comput.*, Vol. **16**, No. 4, pp. 840-847 (1995).
10. R. Scheichl, "Parallel Solver for the Transient Multigroup Neutron Diffusion Equations," Mathematics Preprint 98/30 (1999), University of Bath, United Kingdom; available on the Internet(<http://www.maths.bath.ac.uk/MATHEMATICS/preprints.html>)
11. Rifat M. Al-Chalabi and Paul J. Turinsky, "Application of Multigrid Method to Solving the NEM Form of Multigroup Neutron Diffusion Equation," *Trans. Am. Nucl. Soc.*, **71**, 259 (1994).
12. H. Finnemman, "NEACRP 3D LWR Core Transient Benchmark - Final Specifications," NEACRP-L-335(Revision 1) (1992).
13. R. Fraikin and H. Finnemman, "NEA-NSC 3D/1D PWR Core Transient Benchmark (Uncontrolled Withdrawal of Control Rods at Zero Power) - Final Specifications," OECD/NEA (Sep. 1993).
14. P. R. Engrand, G. I. Maldonado, R. Al-Chalabi, and P. J. Turinsky, "Non-Linear Iteration Strategy for NEM : Refinement and Extension," *Trans. Am. Nucl. Soc.*, **65**, 221 (1992).
15. H. Finnemman, "A consistent Nodal Method for the Analysis of Space-Time Effects in Large LWRs," *Proc. Joint NEACRP/CSNI Specialists' Mtg. on New Developments in Three-Dimensional Neutron Kinetics*, MRR 145, 131, January 22-24, Munich (1975).
16. H. A. Van Der Vorst, "BI-CGSTAB: A fast and smoothly converging variant of BI-CG for the solution of nonsymmetric linear systems," *SIAM J. Sci. Stat. Comput.* **13**, pp. 631-644 (1992).
17. H. Finnemman, H. Bauer, A. Galati and R. Martinelli, "Results of LWR Core Transient Benchmark," NEA/NSC/DOC(93)25 (Oct. 1993).
18. R. Fraikin, "PWR Benchmark on Uncontrolled Rods Withdrawal at Zero Power," NEA/NSC/DOC(96)20 (Sep. 1997).



(a) Fast Transient A1 Case



(b) Slow Transient B Case

Figure 2. Effect of TGC Update Frequency on the Reduction Speed of Residual Norm



Table II. Comparison of nodal CMFD 4 node per assembly Solutions of NEACRP PWR Transient Benchmark Problems

Neutronics Model		Ref. <sup>a</sup>	NEM (E)	NEM (B)	ANM (E)	ANM (B)	Ref. <sup>a</sup>	NEM (E)	NEM (B)	ANM (E)	ANM (B)	Ref. <sup>a</sup>	NEM (E)	NEM (B)	ANM (E)	ANM (B)	
Fast Transient at HFP	problem	Case A2					Case B2					Case C2					
	Initial state	Critical Boron(ppm)	1160.6	1156.1	1154.6	1152.8	1152.0	1189.4	1183.2	1181.6	1179.7	1178.9	1160.6	1156.1	1154.6	1152.8	1152.0
		3D Power Peak(Fq)	2.221	2.215	2.213	2.219	2.217	2.109	2.102	2.100	2.106	2.104	2.221	2.215	2.213	2.219	2.217
	Transient state	Peak Time(s)	0.10	0.110	0.110	0.100	0.110	0.12	0.110	0.120	0.120	0.120	0.10	0.106	0.106	0.106	0.114
		Peak Power	1.080	1.079	1.079	1.080	1.080	1.063	1.065	1.065	1.064	1.064	1.071	1.073	1.072	1.072	1.072
	Final state	Power	1.035	1.035	1.035	1.035	1.035	1.038	1.039	1.039	1.039	1.039	1.030	1.031	1.031	1.031	1.031
	Max. Centerline T.	1691.8	1714.7	1713.8	1719.7	1718.8	1588.1	1604.6	1604.2	1609.1	1608.6	1733.5	1755.8	1754.7	1760.3	1759.1	
	Doppler T.	554.6	557.4	557.5	557.6	557.6	552.0	555.0	554.9	555.0	555.0	553.5	556.5	556.5	556.5	556.5	
	Moderator T.	324.6	326.3	326.3	326.3	326.3	324.7	326.3	326.3	326.3	326.3	324.5	326.2	326.2	326.2	326.2	
	CPU time(s) <sup>b</sup>	-	83.5	59.6	99.5	63.2	-	71.5	49.8	88.3	64.1	-	895.3	560.0	933.2	661.8	
Fast Transient at HZP	problem	Case A1					Case B1					Case C1					
	Initial state	Critical Boron(ppm)	567.7	560.5	560.1	559.3	559.1	1254.6	1250.3	1248.5	1246.1	1245.0	1135.3	1130.4	1128.0	1126.3	1124.8
		3D Power Peak(Fq)	2.874	2.870	2.871	2.880	2.878	1.932	1.925	1.927	1.931	1.931	2.187	2.180	2.179	2.185	2.183
	Transient state	Peak Time(s)	0.56	0.560	0.546	0.540	0.530	0.52	0.505	0.531	0.530	0.535	0.27	0.266	0.272	0.274	0.274
		Peak Power	1.179	1.139	1.211	1.241	1.294	2.441	2.477	2.192	2.193	2.145	4.773	4.457	4.191	4.092	4.097
	Final state	Power	0.196	0.197	0.197	0.197	0.198	0.320	0.324	0.321	0.321	0.321	0.146	0.148	0.147	0.147	0.147
	Max. Centerline T.	673.3	680.2	682.1	684.8	686.4	559.8	572.1	566.8	567.5	566.2	676.1	708.3	702.7	701.9	701.4	
	Doppler T.	324.3	325.4	325.6	325.7	325.9	349.9	352.1	351.3	351.2	351.1	315.9	316.9	316.7	316.6	316.6	
	Moderator T.	293.1	293.4	293.4	293.4	293.4	297.6	298.1	297.9	298.0	297.9	291.5	291.7	291.7	291.7	291.7	
	CPU time(s) <sup>b</sup>	-	800.8	578.5	975.9	708.4	-	566.7	500.5	713.0	644.2	-	5674.1	3965.4	7119.7	4823.7	
Slow Transient at HZP	problem	Case A					Case B					Case D					
	Initial state	Critical Boron(ppm)	1267.7	1264.0	1262.4	1260.2	1259.2	793.6	792.6	791.9	791.1	790.8	793.6	792.6	791.9	791.1	790.8
		3D Power Peak(Fq)	1.880	1.869	1.872	1.881	1.882	2.886	2.875	2.875	2.882	2.880	2.886	2.875	2.875	2.882	2.880
		2D Power Peak(Fxy)	1.242	1.235	1.238	1.244	1.246	1.912	1.904	1.908	1.910	1.912	1.912	1.904	1.908	1.910	1.912
	Transient state	Peak Time(s)	82.14	81.904	81.851	81.634	81.454	34.30	34.200	33.975	34.115	33.918	39.40	38.845	38.750	38.902	38.795
		Peak Power	0.356	0.356	0.356	0.356	0.356	1.348	1.426	1.419	1.441	1.435	0.969	0.978	0.970	0.947	0.950
	Max. Dopplet T.	358.7	361.0	361.3	361.0	361.0	315.2	316.5	316.4	316.5	316.4	312.6	313.4	313.5	313.1	313.1	
	Max. Outlet T.	295.3	299.3	299.3	299.2	299.3	290.5	292.5	292.5	292.5	292.5	290.2	291.9	291.9	291.8	291.8	
	CPU time(s) <sup>b</sup>	-	1059.9	832.0	1256.1	928.7	-	1308.6	1094.0	1556.8	1149.8	-	1124.6	896.5	1313.0	1078.0	

Ref.<sup>a</sup>: H. Finnemman, H. Bauer, A. Galati and R. Martinelli, "Results of LWR Core Transient Benchmark," NEA/NSC/DOC(93)25 (Oct. 1993)

R. Fraikin, "PWR Benchmark on Uncontrolled Rods Withdrawal at Zero Power," NEA/NSC/DOC(96)20 (Sep. 1997)

<sup>b</sup>measured on DEC Workstation(433MHz).

Table III. Comparison of Total CPU Time With and Without Two Grid Correction<sup>a</sup>

Neutronics Model	NEM (E)		NEM (B)		ANM (E)		ANM (B)	
	NC	TGC	NC	TGC	NC	TGC	NC	TGC
A1	800.8(1.00)	674.6(0.84)	578.5(0.72)	483.3(0.60)	975.9(1.00)	899.3(0.92)	708.4(0.73)	600.0(0.61)
A2	83.5(1.00)	68.1(0.82)	59.6(0.71)	39.7(0.48)	99.5(1.00)	84.8(0.85)	63.2(0.64)	52.8(0.53)
B1	566.7(1.00)	516.8(0.91)	500.5(0.88)	422(0.75)	713.0(1.00)	664.6(0.93)	644.2(0.90)	560.8(0.79)
B2	71.5(1.00)	60.0(0.84)	49.8(0.70)	39.5(0.55)	88.3(1.00)	76.0(0.86)	64.1(0.73)	50.9(0.58)
C1	5674.1(1.00)	4770.3(0.84)	3965.3(0.70)	3284.2(0.58)	7119.7(1.00)	6118.3(0.86)	4823.7(0.68)	4111.6(0.58)
C2	895.3(1.00)	729.3(0.81)	560.0(0.63)	416.4(0.47)	933.2(1.00)	849.9(0.91)	661.8(0.71)	515.7(0.55)
A	1059.9(1.00)	859.7(0.81)	832.0(0.78)	625.3(0.59)	1256.1(1.00)	1084.7(0.86)	928.7(0.74)	760.7(0.61)
B	1308.6(1.00)	1094.0(0.84)	950.0(0.73)	729.7(0.56)	1556.8(1.00)	1366.3(0.88)	1149.8(0.74)	869.7(0.56)
D	1124.6(1.00)	965.1(0.86)	896.5(0.80)	643.8(0.57)	1313.0(1.00)	1160.2(0.88)	1078.0(0.82)	868.8(0.66)

<sup>a</sup>The figures in the brackets represent the fraction of CPU time relative to the CPU time spent on CMFD solutions without TGC and CRBC.

Table IV. Comparison of CPU time spent on Iterative Neutronics Calculation With and Without Two Grid Correction<sup>a</sup>

Neutronics Model	NEM (E)		NEM (B)		ANM (E)		ANM (B)	
	NC	TGC	NC	TGC	NC	TGC	NC	TGC
A1	368.9(1.00)	252.8(0.69)	270.1(0.73)	165.6(0.45)	359.4(1.00)	263.0(0.73)	266.6(0.74)	158.2(0.44)
A2	33.8(1.00)	18.3(0.54)	25.4(0.75)	9.1(0.27)	34.0(1.00)	17.3(0.51)	20.9(0.61)	9.5(0.28)
B1	280.7(1.00)	219.6(0.78)	241.5(0.86)	156.5(0.56)	284.4(1.00)	236.0(0.83)	244.2(0.86)	156.1(0.55)
B2	28.7(1.00)	16.7(0.58)	20.9(0.73)	9.6(0.33)	28.7(1.00)	15.9(0.55)	22.0(0.77)	9.4(0.33)
C1	3185.7(1.00)	2156.7(0.68)	2180.1(0.68)	1408.0(0.44)	3303.3(1.00)	2237.6(0.68)	2206.6(0.67)	1436.6(0.43)
C2	475.4(1.00)	289.5(0.61)	290.7(0.61)	143.3(0.30)	412.5(1.00)	258.1(0.63)	291.6(0.71)	142.1(0.34)
A	622.3(1.00)	431.9(0.69)	487.6(0.78)	271.1(0.44)	619.2(1.00)	433.9(0.70)	467.7(0.76)	258.9(0.42)
B	702.3(1.00)	473.0(0.67)	512.4(0.73)	288.4(0.41)	686.1(1.00)	469.4(0.68)	519.4(0.76)	282.6(0.41)
D	646.6(1.00)	461.2(0.71)	509.6(0.79)	280.5(0.43)	629.6(1.00)	447.9(0.71)	511.7(0.81)	288.8(0.46)

<sup>a</sup>The figures in the brackets represent the fraction of CPU time relative to the CPU time spent on CMFD solutions without TGC and CRBC.